Initializing the flux state of multiwell inductively isolated Josephson junction qubits

T. A. Palomaki, S. K. Dutta, Hanhee Paik, H. Xu,* J. Matthews, R. M. Lewis, R. C. Ramos,† K. Mitra, Philip R. Johnson,‡ Frederick W. Strauch,‡ A. J. Dragt, C. J. Lobb, J. R. Anderson, and F. C. Wellstood

Center for Superconductivity Research, Department of Physics, University of Maryland, College Park, Maryland 20742-4111, USA

(Received 19 August 2005; revised manuscript received 6 December 2005; published 24 January 2006)

We describe a technique for initializing the flux state of an inductively isolated Josephson junction, fulfilling an essential requirement for using the device as a qubit. By oscillating the applied magnetic flux with a specified amplitude and offset, we can select any of the allowed long-lived metastable flux states. We applied this technique to Nb-Al_2O_3-Nb and Al-Al_2O_3-Al devices with from 10 to over 100 distinct flux states at temperatures as low as 25 mK. In a ten-state system with an initial probability $p=0.13$ to be in the desired flux state, we achieved $p=0.999\,96$ after 50 oscillations at 22.6 kHz. The technique is generally applicable to other systems with multiple metastable wells (including rf SQUIDs), requires no additional readout or bias lines, involves minimal energy dissipation, and appears to scale favorably with the number of qubits.

DOI: 10.1103/PhysRevB.73.014520 PACS number(s): 74.50.+r, 03.67.Lx, 85.25.Cp, 85.25.Dq

In order to be used as a qubit in a quantum computer, a physical system must satisfy the DiVincenzo criteria.[1,2] Perhaps the most basic of these criteria is that one must be able to prepare the system in a well-defined initial state. This simple requirement has had a major impact on the design of qubits based on Josephson junctions.[3–13] For example, much recent work has been reported on quantum coherence and other quantum effects in single junction rf SQUIDs[3–5] and three-junction SQUIDs.[7–9] In each of these devices, the critical currents of the junctions and the loop inductance were chosen so that the system acts as a particle moving in a two-well potential rather than in a potential with three or more local minima; thereby allowing a simple initialization process. Removing the two-well constraint for initialization would allow for a far wider range of system parameters, and thus more design flexibility.

In multiwell systems, the different minima of the potential correspond to different amounts of total flux and persistent current in the SQUID loop. Within each well, the system can have well-localized eigenstates; a subset of these states forms the computational basis states for the qubit (see Fig. 1). For two-well potentials, the flux state of the system can be initialized by applying a magnetic flux that causes one of the wells to become unstable, leaving just one well for the system to occupy. This simple process does not work if the potential has more than two wells; in this case, the system can end up via a random process in any well with lower energy, causing a random final flux state.

Despite the perceived difficulty of initializing systems with multiple metastable levels, Martinis *et al.* recently reported measurements on an inductively isolated Josephson junction,[10] a system that we will show naturally tends to have multiple nonequivalent flux states. For typical operating conditions the different flux states are extremely long-lived. We note that, in principle, a flux detector could be used to determine the flux state and the trapped flux then forced to change by the application of an external flux until the desired flux state is reached.[5] However, this type of qubit does not ordinarily include a flux detector (the state is measured by finding the current at which the system tunnels to the voltage state), and the addition of a flux detector would seriously complicate the device.

More than a decade ago, Lefevre-Seguin *et al.*[14] reported an altogether different approach to initializing the flux state of a dc SQUID that does not require a flux sensor. In this paper, we present a variation on their "forced-retrapping" scheme that is well suited for initializing the flux state of inductively isolated Josephson junction qubits at mK temperatures. We also examine the factors that lead to multiple states, describe results for devices with different numbers of possible flux states, and conclude with a discussion of scaling and some implications for quantum computation.

Figure 2(a) shows a schematic of an inductively isolated Josephson junction qubit. The qubit (junction 1) is placed in series with a relatively large inductor L_1, and this combination is placed in parallel with a small inductor L_2 and an isolation junction (junction 2).[10] This configuration forms a current divider yielding broadband isolation of the qubit junction from current noise, a source of decoherence.[13] An examination of the schematic reveals that the device is simply a dc SQUID with an inductive and critical current

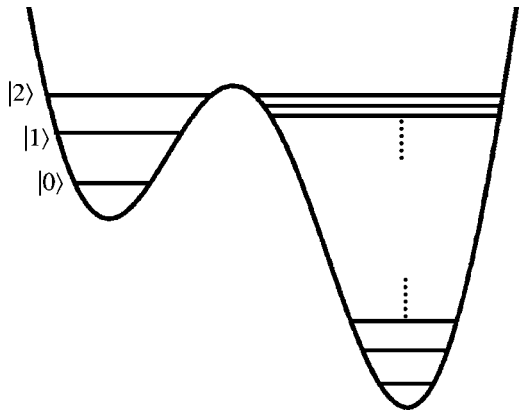

FIG. 1. Sample potential energy curve for a two-well system. Energy eigenstates are shown that form the computational basis states of the qubit. Flux shaking allows systems with more than two potential wells to be investigated as qubits.

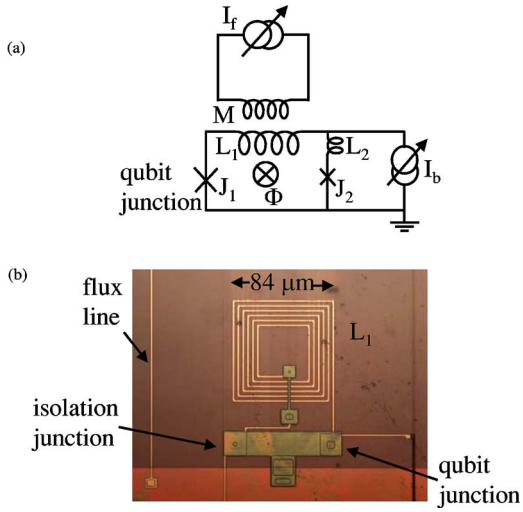

FIG. 2. (Color online) (a) Circuit diagram for the inductively isolated Josephson junction qubit or asymmetric dc SQUID. The small junction and inductors L_1 and L_2 isolate the qubit junction from bias current noise. (b) Photograph of Nb SQUID, device A. The square spiral coil is inductor L_1.

asymmetry.[15] The behavior of the system is analogous to a ball moving in a two-dimensional (2-D) corrugated potential (see Fig. 3) and the qubit states are formed by the energy levels in a potential well.

By ramping the bias current I_b and flux Φ_a applied to the loop simultaneously in the proper proportion, the current through each junction can be independently controlled. The state of the qubit can be read out with the same technique used for conventional current-biased Josephson junction qubits,[10,12] i.e., by observing the rate at which the qubit tunnels to the finite-voltage state from the zero-voltage state. Since a purely inductive isolation network would short out any dc voltage developed across the qubit junction, an "isolation junction" (junction 2) is added to the shunting arm of the network. With suitable choices of parameters, when the qubit switches, the isolation junction will also switch into the finite voltage state, thereby producing a steady voltage that can be detected on the leads.

To understand why the inductively isolated junction qubit

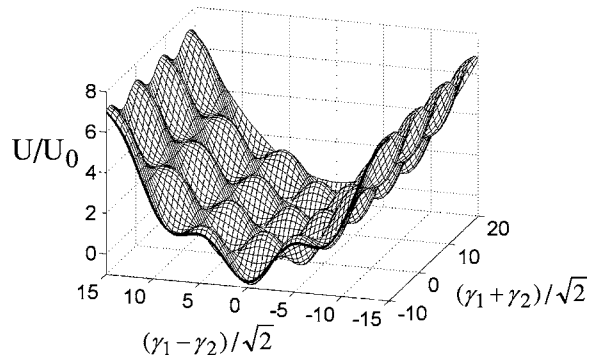

FIG. 3. Normalized potential energy surface $U(\gamma_1,\gamma_2)/U_0$, where $U_0=I_0\Phi_0/\pi$, for current $I_b=0$, flux $\Phi_a=0$, $\beta=5.3$, and $I_0=I_{01}=I_{02}$. This sample potential clearly shows how many potential wells exist for a dc SQUID.

tends to have multiple metastable flux states, first note that the system involves two inductively coupled junctions. In order to treat the qubit junction as a single well-isolated quantum system with one degree of freedom (the phase difference γ_1 across the qubit junction), this degree of freedom must not be strongly coupled to that of the isolation junction (with its degree of freedom being the phase difference γ_2 across the isolation junction). The Hamiltonian for the system is[16]

$$H=\frac{p_1^2}{2m_1}+\frac{p_2^2}{2m_2}+U(\gamma_1,\gamma_2,I_b,\Phi_a), \tag{1}$$

where

$$U(\gamma_1,\gamma_2,I_b,\Phi_a) = -E_{J1}\cos(\gamma_1)-E_{J2}\cos(\gamma_2)-\left(\frac{\Phi_0 I_b}{2L\pi}\right) \times(L_2\gamma_1+L_1\gamma_2)+\left(\frac{\Phi_0}{2\pi}\right)^2\frac{1}{2L}\left(\gamma_1-\gamma_2-\frac{2\pi\Phi_a}{\Phi_0}\right)^2. \tag{2}$$

Here $p_1=C_1(\Phi_0/2\pi)^2\dot{\gamma}_1\equiv m_1\dot{\gamma}_1$ and $p_2=C_2(\Phi_0/2\pi)^2\dot{\gamma}_2\equiv m_2\dot{\gamma}_2$ are the canonical momenta, L_1 and L_2 are the geometrical inductances of the left and right arms, $L=L_1+L_2$ is the total loop inductance, C_1 and C_2 are the capacitances of the qubit and isolation junctions, I_{01} and I_{02} are the critical currents of the qubit and isolation junctions,Φ_a is the applied flux coupled into the loop, Φ_0 is the flux quantum, and $E_{J1}=I_{01}\Phi_0/2\pi$ and $E_{J2}=I_{02}\Phi_0/2\pi$ are the Josephson coupling energies of the two junctions.

To lowest order, we can approximate the system as two coupled harmonic oscillators. Expanding the coupled Hamiltonian about a potential minimum and finding the normal modes gives a resonant plasma frequency ω_1. In this case, inductively coupling two junctions together will produce a fractional shift in the resonant frequency of the qubit junction given by[17]

$$\kappa=|(\omega_1-\omega_{p1})/\omega_{p1}|\approx\omega_0^4/2(\omega_{p2}^2-\omega_{p1}^2)\omega_{p1}^2, \tag{3}$$

where $\omega_0^4\equiv 1/(L^2C_1C_2)$, $\omega_{p2}>\omega_{p1}$ (as in typical operation), and the shift is small compared to ω_{p1}. The resonant plasma frequencies of the uncoupled junctions are ω_{p1} and ω_{p2}.[14] The frequency shift is a measure of the dynamical coupling between the devices. For the two junctions to act independently, we require $\kappa\ll 1$.

Equation (3) can be written in the form

$$\kappa\cong 2/[(2\pi\beta)^2(1-\alpha^2)\sqrt{1-(I_1/I_{01})^2}], \tag{4}$$

where I_1 is the current through the qubit junction, $\alpha=(I_{02}-I_{01})/(I_{02}+I_{01})$, and $\beta=L(I_{01}+I_{02})/\Phi_0$ is the SQUID modulation parameter.[15] Thus, $\kappa\ll 1$ implies

$$\beta\gg\frac{1}{2\pi}\sqrt{\frac{2}{1-\alpha^2}}\frac{1}{[1-(I_1/I_{01})^2]^{1/4}}. \tag{5}$$

We note that Eq. (5) is not what one would find by simply examining the Hamiltonian and taking the ratio of the energy terms.[14] Expanding the last term in Eq. (2) reveals a coupling

TABLE I. Parameters for an inductively isolated Josephson junction (SQUID) for device A and device B. L_1 and L_2 are the geometrical inductance of the left and right arm of the SQUID loop, respectively, I_{01} is the qubit critical current, I_{02} is the isolation junction critical current, A_1 and A_2 are the qubit and isolation junction areas, respectively, M is the mutual inductance between the flux line and the SQUID loop, L_{j1} and L_{j2} are the unbiased Josephson inductances of the qubit and isolation junction (with no current), respectively, $r=[(L_1+L_{j1})/(L_2+L_{j2})]^2$ is the dc rejection ratio, C_1 and C_2 are the capacitances of the qubit and isolation junction respectively, $\beta=L(I_{01}+I_{02})/\Phi_0$, and N_Φ is the total number of flux states experimentally detected.

	Device A	Device B
Fabrication	Hypres	UMD
Material	$Nb/Al_2O_3/Nb$	$Al/Al_2O_3/Al$
I_{01} (μA)	33.8 (88 unsuppressed)	24.9
I_{02} (μA)	4.8 (48 unsuppressed)	7.4
A_1	10 μm$\times$10 μm	2 μm$\times$40 μm
A_2	7 μm$\times$7μm	2 μm$\times$20 μm
M (pH)	51.2	16.4
L_1 (nH)	3.53	1.23
L_2 (pH)	20	12
L_{j1} (pH)	9.7 (3.7 unsuppressed)	13.2
L_{j2} (pH)	68 (6.8 unsuppressed)	44.7
r	1.6×10^3 (2×10^4)	4.8×10^2
C_1 (pF)	4.4	4.1
C_2 (pF)	2.2	2.1
β	67 (234 unsuppressed)	20
N_Φ	16 (167 unsuppressed)	10

energy of $-(\Phi_0/2\pi)^2\gamma_1\gamma_2/L$ between the two junctions. With the overall energy scale set by $E_{j1}+E_{j2}$, this suggests a dimensionless coupling strength of $\kappa_0=1/(2\pi\beta)$. Therefore $\kappa_0\ll1$ and thus $\beta\gg1/2\pi$ is required in order for the two junctions to be weakly coupled[14] rather than the constraint $\kappa\ll1$, as given by Eq. (4). Although Eq. (5) may appear to be even more restrictive than the naïve condition, it is, in fact, less restrictive since the coupling is set by $\kappa\propto1/\beta^2$ rather than $\kappa_0\propto1/\beta$.

In the weak-coupling limit the junctions act independently and the maximum current circulating in the loop will be limited by the smaller of the two junction critical currents. Martinis *et al.* chose the critical current of the isolation junction to be about one-half that of the qubit,[10] and we followed this same design. In this case, the number of metastable flux states is

$$N_\Phi \cong 1 + 2LI_{o2}/\Phi_o \approx 1 + \beta(1+\alpha), \tag{6}$$

with $\alpha\approx-1/3$. The first term accounts for a state with no trapped flux, and the factor of 2 accounts for states corresponding to positive and negative circulating current. Thus devices with $\beta\gg1$ will have $N_\Phi\gg1$. For example, one of our devices (see device B in Table I) has $I_{01}+I_{02}=32.3$ μA, $\alpha\approx-0.54$, $L=1.24$ nH, $C_1=4.1$ pF, $C_2=2.1$ pF, and typically we operate at $\omega_{p1}\approx2\pi\times7$ GHz and $\omega_{p2}\approx2\pi\times20$ GHz. In this case one finds $\omega_0=2\pi\times3$ GHz, $\beta=19$, $\kappa_0=1/2\pi\beta=8.2\times10^{-3}$, and $\kappa=1.2\times10^{-3}$. This device is clearly in the weak coupling limit, and κ is almost an order of magnitude smaller than κ_0. For this device, Eq. (6) predicts $N_\Phi\approx10$ flux states.

Our approach to selecting one flux state out of the N_Φ possible states is an extension of Lefevre-Seguin's "forced-retrapping" scheme.[14] They apply an oscillating bias current I_b to the hysteretic SQUID with a maximum that is somewhat less than $I_{01}+I_{02}$, the critical current of the SQUID. If flux is trapped in the loop, a static circulating current will be present that adds current to one junction and subtracts it from the other. If the net current from the bias and trapped flux exceeds the critical current of one of the junctions, the device switches to the finite voltage state and then retraps into another flux state once I_b decreases below the retrapping current. By choosing the amplitude of I_b correctly, all of the flux states can be made unstable, except for the state corresponding to zero trapped flux. Since each cycle that the system is in an undesired state it is forced to retrap into another allowed flux state, which is not necessarily the desired one, Lefevre-Seguin *et al.* applied many current oscillations to ensure that the probability of reaching the selected state was near unity.

In our technique, instead of applying an oscillating current, we apply a sinusoidal oscillating flux to the SQUID. By also applying a static flux, our "flux-shaking" technique allows us to choose *any* one of the allowed flux states, as opposed to only the state needing the most bias current to switch to the voltage state. Moreover, the technique resets the flux state with minimal energy release, since switching to the voltage state only occurs for extremely brief intervals. In the Lefevre-Seguin method the system is in the voltage state until the oscillating current forces it to retrap. Energy considerations are important because we operate our qubits at 25 mK, and significant heating occurs when a junction is in the finite voltage state.

To gain insight into both techniques, consider the potential energy $U(\gamma_1,\gamma_2,I_b,\Phi_a)$ given by Eq. (2), for the simple case of a symmetric SQUID with $\beta=5.3$, when $I_b=0$ and $\Phi_a=0$ (see Fig. 3). There is a degeneracy due to the periodicity of the potential in the $(\gamma_1+\gamma_2)/\sqrt{2}$ direction, and the physically distinct flux states occur at the minima of the wells with minima at different $(\gamma_1-\gamma_2)/\sqrt{2}$. In the current shaking technique, increasing the bias current tilts the potential in the $(\gamma_1+\gamma_2)/\sqrt{2}$ direction. Wells of higher potential have larger $|(\gamma_1-\gamma_2)/\sqrt{2}|$, and lower barrier heights, and thus become unstable at a lower bias current. In the flux-shaking technique, increasing the flux effectively shifts the potential in the $(\gamma_1-\gamma_2)/\sqrt{2}$ direction, changing which flux state corresponds to the minimum potential energy. Again, wells corresponding to stable states can become unstable while previously unstable states can become stable; the total number of stable states will not change in the large β limit. We note that for $I_b=0$, the potential, and thus the flux-shaking process, does not depend on the inductive asymmetry of the SQUID.

If the system is at a minimum that becomes unstable due to the applied current or flux, there are two distinct options: The system can retrap in another stable well, producing a

short-lived voltage (undetectable to us), or it can roll continuously in the $(\gamma_1+\gamma_2)/\sqrt{2}$ direction, producing a steady measurable voltage, until the current through the junction drops below the retrapping current. By using the bias current to make a potential well unstable the system stays in the finite voltage state until the current falls below the retrapping current. On the other hand, if the system is in a potential well that becomes unstable due to a change in flux with $I_b=0$, it escapes and must always retrap in another well, just releasing the difference in energy between the original and final state.

To choose just one flux state using our technique, we make all but the desired well unstable at some point during each flux oscillation. In this way if the system is trapped in an undesired well, this well becomes unstable at some point in each cycle, and the system will be forced to choose a new well. If it happens to retrap in the desired well, then it will be trapped there for the remainder of the oscillations since this one desired state is always stable. If the system lands in any other well, then during the next oscillation it will again be forced out and we have to find a new flux state. Although the retrapping is random, the probability of being in the wrong well decreases exponentially with the number of oscillations; very low failure rates can be achieved with relatively few oscillations (50–100). Different flux states can be selected by applying an appropriate static flux so that the desired well has the lowest energy.

We used the flux-shaking method on two different devices (see Table I). Device A [see Fig. 2(b)] was made from a 100 A/cm^2 (critical current/area) Nb-Al_2O_3-Nb trilayer.[18] The qubit junction's area is 10 $\mu m \times 10$ μm, but the critical current was suppressed to about 33.8 μA by applying a parallel magnetic field. Device B was fabricated in our lab from Al-Al_2O_3-Al and the qubit junction had a critical current of 24.9 μA. Double layer photolithography was used to define the device pattern and double angle evaporation was used to create the junctions and on-chip wiring. The Al-based and Nb-based devices produced similar data for each measurement and technique applied.

For testing, device A was mounted in a superconducting Al box that was connected to the mixing chamber of an Oxford Instruments model 200 dilution refrigerator with a base temperature of about 25 mK. Device B was mounted in vacuum in a superconducting Al box that was connected to the mixing chamber of an Oxford Instruments Kevinox-50 dilution refrigerator with a base temperature of about 80 mK. In both cases all lines were filtered using custom rf and microwave Cu powder filters.[19]

Both devices were characterized electrically by measuring the switching current (the current at which the device switches to the finite voltage state) as a function of applied flux (see Fig. 4, which shows data for device B). As expected the device shows multiple allowed flux states; for any given applied flux, switching occurred at multiple currents (corresponding to different amounts of trapped flux) separated by approximately $\Delta I_b=\Phi_0/L$. We note also that Fig. 4 shows the presence of steep branches with a negative slope equal to $1/(L_2+L_{2J})$, and more gradual positive slope branches, with a slope equal to $1/(L_1+L_{1J})$, where L_{2J} and L_{1J} are the kinetic inductance of the junctions. The steep branches correspond to the qubit junction switching to the voltage state

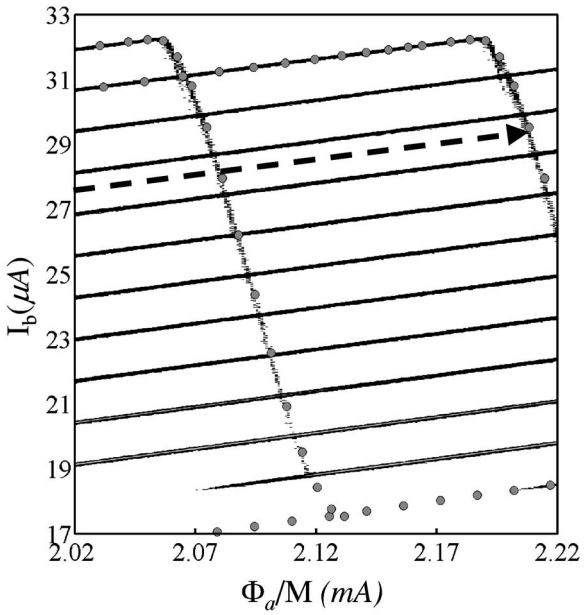

FIG. 4. Bias current I_b at which switching occurs versus current applied to flux modulation coil $I_f=\Phi_a/M$ for device B measured at 80 mK. The z axis represents histogram counts where the system switches to the voltage state. Grey circles show a theoretical fit using parameters in Table I for device B. The dashed arrow shows a sample trajectory such that only the qubit junction may switch to the voltage state first.

first, while for the gradually sloped branch the isolation junction switches first. The highest bias current where a switch occurs is $I_{c1}+I_{c2}$ and corresponds to the flux being such that both junctions switch simultaneously. The values for the inductances and critical currents in Table I were found by fitting simulations to the experimental curves[20] (see Fig. 4).

The asymmetry of the critical currents in device B can be seen in its potential (see Fig. 5). Once again, increasing the flux effectively shifts the potential in the $(\gamma_1-\gamma_2)/\sqrt{2}$ direction and if the system becomes unstable with no bias current it will quickly retrap. By ramping I_b and Φ_a at the proper ratio this potential can be tilted such that the system can only escape in the γ_1 direction, corresponding to the qubit junction switching first.

Before performing the initialization procedure, we determined the probability of finding the system in each flux state.

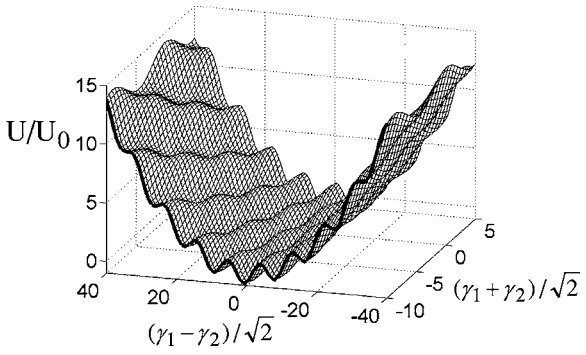

FIG. 5. Normalized potential energy surface $U(\gamma_1,\gamma_2)/U_0$ for device B, where $U_0=I_0\Phi_0/\pi$.

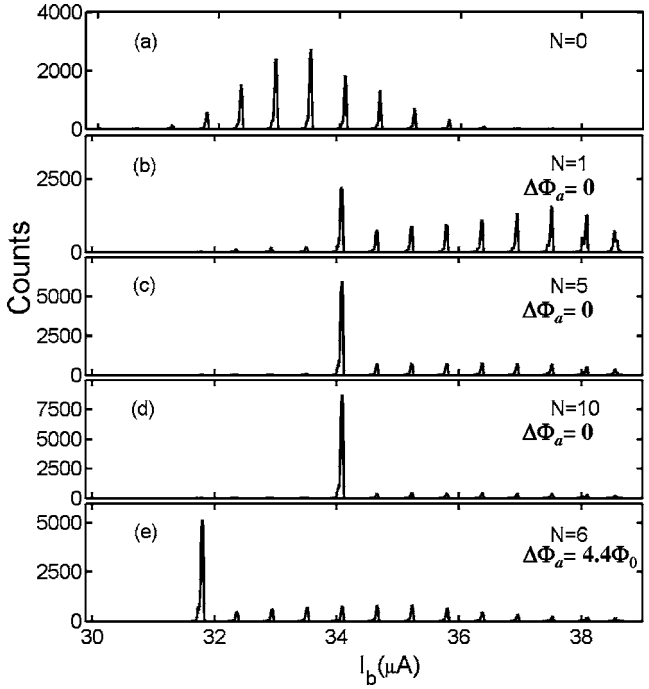

FIG. 6. (a) Initial switching histogram, for device A at 25 mK. (b) Switching histogram after $N=1$ oscillations; (c) $N=5$ oscillations; and (d) $N=10$ oscillations of amplitude $7.4\Phi_0(I_f=0.3$ mA) at 44 kHz. For (b)–(d), no flux offset was applied, and the $n=0$ state was selected. (e) Isolating the $n=-4$ flux state using $N=6$ oscillations of amplitude $7.4\Phi_0$, at 44 kHz and with a flux offset of $4.4\Phi_0(I_f=0.177$ mA).

We ramped the bias current and flux such that only the qubit junction switches first and a minimal amount of bias current passes through the isolation junction. A sample trajectory is shown as the dashed arrow in Fig. 4. This simultaneous sweep of current and flux was repeated every 5 ms to build up a histogram of the bias current at which the junction switched to the voltage state. After each ramp, I_b and Φ_a were set to zero, forcing the system to retrap randomly in an allowed flux state. The $n=0$ flux state may not be the most probable when retrapping from the voltage state if any applied flux is present when it retraps. By summing the counts in each peak of the histogram, we can determine the starting probability of being in each well. Figure 6(a) shows the initial histogram for device A at 25mK.

To set the system in a specific well using flux shaking, we chose a number of oscillations N, flux offset, and flux oscillation amplitude and then applied the flux at a fixed frequency (44 kHz in this experiment) until N oscillations were completed. Any frequency below the bandwidth limit of our filters was effective in our technique. After waiting an arbitrary time, we then measured the switching current, and repeated this entire process to build up histograms for each set of conditions. Each amplitude, flux offset, and number of oscillations produced a different histogram. For a specific range of amplitudes, centered at $N_\Phi\Phi_0/2$, and offsets, it is possible to make every well unstable at some point in the oscillation, except one chosen well. Applying more oscillations in this case produces a steady increase in the probability p_n of finding the system in the desired flux state n [see Figs. 6(b)–6(d)]. Increasing the amplitude further results in no continuously stable state during the initialization process, and no single peak develops an increasing probability. The offset value $\Delta\Phi_a$ of the oscillation determines which peak becomes heavily populated. In Figs. 6(b)–6(d), no flux offset was applied, and the $n=0$ state was selected using flux oscillations of amplitude of $7.4\Phi_0$. In Fig. 6(e) we applied a flux offset of $4.4\Phi_0$ to select the $n=-4$ state.

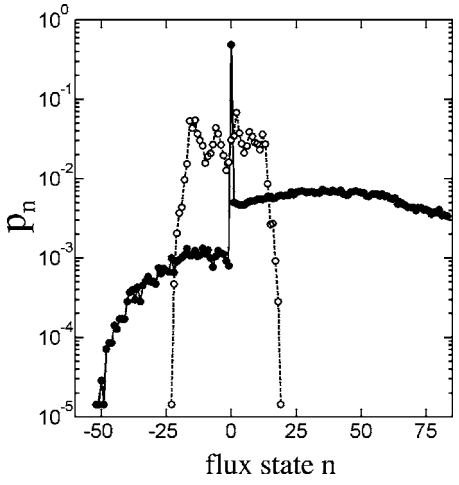

FIG. 7. The zero flux state selected in device A using $N=45$ oscillations of amplitude 3.37 mA ($83.4\Phi_0$) and $f=20$ kHz shown by solid dots. In this case the critical currents were unsuppressed and the device had 167 states. The dashed line shows the initial probabilities (p_n).

We note that during flux shaking of device A, flux states appeared at bias currents of 38 and 38.5 μA [see Fig. 6(b)], while no such states were evident in the original switching distribution [see Fig. 6(a)]. Evidently, these states are stable states of the system, but had a negligible probability of being occupied due to retrapping from the voltage state. For certain flux values during the final flux oscillation, these states have a substantially higher probability of becoming occupied. Since they are stable states with no applied flux, they can remain populated.

We also tested device A when its critical current was not suppressed. In this case the critical current was an order of magnitude higher, and we found 167 flux states. We found that the initial probability of occupying the $n=0$ well (corresponding to no circulating current) was $p_0=0.03$. Figure 7 shows that after 45 oscillations we could increase this to $p_0=0.493$.

To use such a device as a qubit, ultimately one will need to initialize the system with near-unity probability. Figure 8 shows how the failure rate $q_0=1-p_0$ for selection of the $n=0$ state for device B falls with the number of oscillations for up to 50 oscillations. By 50 oscillations, the probability of being in the desired state, which is initially $p_0=0.13$, increases to $p_0=0.999\,96$. For this measurement we chose the oscillation frequency so that the entire initialization procedure always took 2.2 ms, independent of the number of oscillations; e.g., a frequency of 22.6 kHz was used for 50 oscillations. As expected, the failure probability decreases exponentially with the number of oscillations. More oscilla-

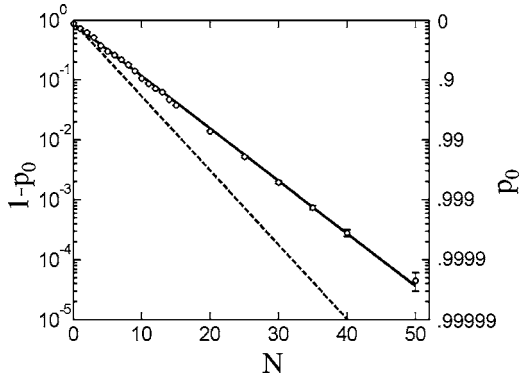

FIG. 8. Probability ($q_0=1-p_0$) of *not* occupying the $n=0$ state versus the number of flux oscillations N, showing the exponential decay of $1-p$ with N for device B at 80 mK. For each point, 2×10^5 cycles of initialization and readout were performed. The dashed line shows simulation results based on the initial distribution. The solid line is an exponential fit to the data.

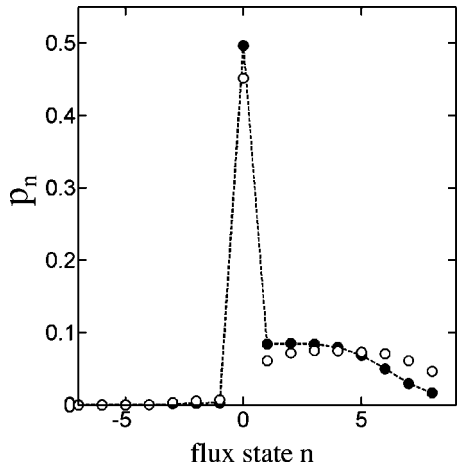

FIG. 9. Probability of occupying different allowed flux states after four oscillations for device A. Simulations (dashed lines) and data (open circles) after four oscillations in device A.

tions are clearly possible; extrapolating the trend to 100 oscillations implies $1-p$ would fall to about 2×10^{-9}.

To understand the switching histograms produced by flux shaking, we developed a simple model for this process. When a change in the flux makes the system unstable, we assume it will retrap in the stable states with the same probability as the initial distribution [see, e.g., Fig. 6(a)], except shifted by the applied flux. This model naturally causes $1-p$ to decrease exponentially with N for the desired well (see the dashed line in Fig. 8). Figure 9 shows a comparison between the measured probability for each well and this simple model for four oscillations of device A. While we find reasonable qualitative agreement for small N, significant differences arise for large N, most likely because the retrapping probability is not identical to the initial probability distribution.

To be useful in a quantum computer where N_q qubits are coupled together, the time to initialize the entire system must not grow faster than a polynomial in N_q. While here we only report experimental results on single qubits, the situation for multiple coupled qubits appears favorable. In principle, if the resetting of one qubit does not disturb the state of the others, then the same flux oscillation could be supplied to every qubit at the same time. By way of example, suppose that $N=100$ oscillations will set the state of one qubit with a probability $p=1-q=1-10^{-6}$. Then the probability that all of $N_q=1000$ qubits are set to the correct initial state after 100 oscillations will be $p\sim1-N_qq=1-10^{-3}\sim1$. Since the one-qubit probability of failure q decreases exponentially with the number of oscillations N, reducing the failure rate of N_q to a set level only requires increasing N logarithmically with N_q. Although resetting one qubit may disturb the state of others, particularly nearest neighbors, most qubit schemes involve relatively weak qubit-qubit coupling, suggesting that a little disturbance will be created.

More energy would be produced if two neighbors of a qubit reset at the same time. While this would be a relatively rare occurrence, it could be prevented by first applying flux oscillations to every other qubit (each qubit has two neighbors that are not being reset), and then applying oscillations to the remaining devices. This would increase the time to initialize the entire system by a factor of 2, independent of the total number of qubits.

In conclusion, by applying oscillating flux to an inductively isolated Josephson junction we have shown how to initialize its flux state. The technique is efficient, rapid, involves minimal energy dissipation, and does not require additional wiring or detection. Thus, insofar as the state initialization is concerned, there is no need to require that a system have only two wells to be useful as a qubit. The technique is clearly applicable to rf SQUIDs and three junction SQUIDs with many metastable states, and systems with a far wider range of parameters can be investigated as qubits than has generally been recognized. Experiments are now underway to test the scaling of this technique with the number of qubits; preliminary results indicate the technique works for two coupled qubits.

F.C.W. would like to thank C. Urbina for conversations at SQUID'91 concerning their group's technique for setting the flux state of a hysteretic SQUID,[14] a result that was central to the work reported here. We would like to thank the referees for their very helpful comments. Finally, we acknowledge support from the National Science Foundation through the QuBIC Program, the National Security Agency, and the state of Maryland through the Center for Superconductivity Research.

*Present address: School of Applied Physics, Cornell University, Ithaca, New York 14853, USA.
†Present address: Department of Physics, Drexel University, Philadelphia, Pennsylvania 19104, USA.
‡Present address: NIST Physics Laboratory, Gaithersburg, Maryland 20899, USA.

[1] D. P. DiVincenzo, Fortschr. Phys. **48**, 771 (2000).
[2] R. Hughes *et al.*, "A quantum information science and technology roadmap," version 2.0, April 2004, http://qist.lanl.gov
[3] J. R. Friedman, V. Patel, W. Chen, S. K. Tolpygo, and J. E. Lukens, Nature (London) **406**, 43 (2000).
[4] S. Han, Y. Yu, X. Chu, S.-I. Chu, and Z. Wang, Science **293**, 1457 (2001).
[5] R. McDermott, R. W. Simmonds, M. Steffen, K. B. Cooper, K. Cicak, K. D. Osborn, S. Oh, D. P. Pappas, and J. M. Martinis, Science **307**, 1299 (2005).
[6] A. J. Leggett, Prog. Theor. Phys. **69**, 80 (1980).
[7] C. H. van der Wal, A. C. J. ter Haar, F. K. Wilhelm, R. N. Schouten, C. J. P. M. Harmans, T. P. Orlando, S. Lloyd, and J. E. Mooij, Science **290**, 773 (2000).
[8] I. Chiorescu, Y. Nakamura, C. J. P. M. Harmans, and J. E. Mooij, Science **299**, 1869 (2003).
[9] B. L. T. Plourde, T. L. Robertson, P. A. Reichardt, T. Hime, S. Linzen, C.-E. Wu, and J. Clarke, Phys. Rev. B **72**, 060506(R) (2005).
[10] J. M. Martinis, S. Nam, J. Aumentado, and C. Urbina, Phys. Rev. Lett. **89**, 117901 (2002).
[11] R. W. Simmonds, K. M. Lang, D. A. Hite, S. Nam, D. P. Pappas, and J. M. Martinis, Phys. Rev. Lett. **93**, 077003 (2004).
[12] R. C. Ramos, M. A. Gubrud, A. J. Berkley, J. R. Anderson, C. J. Lobb, and F. C. Wellstood, IEEE Trans. Appl. Supercond. **11**, 998 (2001).
[13] H. Xu, A. J. Berkley, R. C. Ramos, M. A. Gubrud, P. R. Johnson, F. W. Strauch, A. J. Dragt, J. R. Anderson, C. J. Lobb, and F. C. Wellstood, Phys. Rev. B **71**, 064512 (2005).
[14] V. Lefevre-Seguin, E. Turlot, C. Urbina, D. Esteve, and M. H. Devoret, Phys. Rev. B **46**, 5507 (1992).
[15] C. D. Tesche and J. Clarke, J. Low Temp. Phys. **29**, 301 (1977).
[16] F. Strauch, Ph.D. thesis, University of Maryland, College Park, 2005, p. 48.
[17] F. Wellstood *et al.* (unpublished).
[18] Fabricated by Hypres, Inc., Elmsford, New York.
[19] K. Bladh, D. Gunnarsson, E. Hurfeld, S. Devi, C. Kristoffersson, B. Smalander, S. Pehrson, T. Claeson, P. Delsing, and M. Taslakov, Rev. Sci. Instrum. **74**, 1323 (2003).
[20] W. Tsang and T. Duzer, J. Appl. Phys. **46**, 4573 (1975).